REVISTA DCS
FUNDADA EN 2000

COORDINATED MULTI-LAYER VOLTAGE CONTROL WITH PREDICTIVE TAP SCHEDULING FOR ACTIVE DISTRIBUTION NETWORKS

CONTROLE COORDENADO DE TENSÃO EM MÚLTIPLAS CAMADAS COM PROGRAMAÇÃO PREDITIVA DE DERIVAÇÕES PARA REDES DE DISTRIBUIÇÃO ATIVAS

CONTROL COORDINADO DE TENSIÓN MULTICAPA CON PROGRAMACIÓN PREDICTIVA DE TOMAS PARA REDES DE DISTRIBUCIÓN ACTIVAS

Weverson dos Santos Cirino[1], Thiago Mota Soares[2], Israel Gondres Torné[3]

DOI: 10.54899/dcs.v23i94.6832
Recibido: 31/07/2026 | Aceptado: 24/08/2026 | Publicación en línea: 31/08/2026.

ABSTRACT

Active distribution networks with high penetration of PV, BESS, and EV charging face significant voltage regulation challenges and accelerated OLTC wear. This paper proposes a coordinated multi-layer voltage control framework operating across multiple time scales. It integrates fast local fuzzy Volt–Var and state-of-charge–aware P/Q control at the inverter/BESS level, intermediate coordinated capacitor switching, and a supervisory OLTC scheduler formulated as a model predictive control (MPC) problem. The resulting hybrid continuous–discrete closed-loop system is evaluated via time-domain co-simulation on a modified IEEE 13-bus feeder (IEEE 13-bus+SFVE) and a real 150-bus urban feeder in Manaus (RDRM), under realistic irradiance and load profiles. For the IEEE 13-bus+SFVE, the scheme reduced feeder-wide voltage violations from 15.22% to 4.83% and OLTC tap operations from 14 to 1 per day. For the RDRM feeder, violations dropped from 72.44% to 9.76%, with only one OLTC operation over 24 hours, both without PV curtailment. This integrative contribution demonstrates substantial improvements in volt-age quality and OLTC lifespan, highlighting a practical pathway for active distribution network management.

Keywords: Voltage Control. Distribution Networks. Electric Vehicles. OLTC. Photovoltaic.

RESUMO

Redes de distribuição ativas com alta penetração de sistemas fotovoltaicos (PV), sistemas de armazenamento de energia por bateria (BESS) e recarga de veículos elétricos (EV) enfrentam desafios significativos de regulação de tensão e desgaste acelerado do OLTC. Este artigo propõe uma estrutura coordenada de controle de tensão em múltiplas camadas, operando em diversas

[1] Ph.D. candidate in Electrical Engineering, Universidade Federal do Pará, Belém, Pará, Brazil.
E-mail: weverson.cirino@itec.ufpa.br
[2] Ph.D. in Electrical Engineering, Universidade Federal do Pará, Belém, Pará, Brazil.
E-mail: thiagosoares@ufpa.br
[3] Ph.D. in Electrical Engineering, Universidade do Estado do Amazonas, Manaus, Amazonas, Brazil.
E-mail: itorne@uea.edu.br

escalas de tempo. Ela integra controle local rápido do tipo “Volt–Var” com lógica difusa e controle P/Q sensível ao estado de carga no nível do inversor/BESS, comutação coordenada intermediária de capacitores e um programador de supervisão do OLTC formulado como um problema de controle preditivo de modelo (MPC). O sistema híbrido de malha fechada contínuo-discreto resultante é avaliado por meio de co-simulação no domínio do tempo em um alimentador IEEE de 13 barramentos modificado (IEEE 13-bus+SFVE) e em um alimentador urbano real de 150 barramentos em Manaus (RDRM), sob perfis realistas de irradiância e carga. Para o alimentador IEEE de 13 barramentos+SFVE, o esquema reduziu as violações de tensão em todo o alimentador de 15,22% para 4,83% e as operações de ajuste do OLTC de 14 para 1 por dia. Para o alimentador RDRM, as violações caíram de 72,44% para 9,76%, com apenas uma operação do OLTC em 24 horas, ambas sem restrição da geração fotovoltaica. Esta contribuição integrativa demonstra melhorias substanciais na qualidade da tensão e na vida útil do OLTC, destacando um caminho prático para o gerenciamento ativo da rede de distribuição.

Palavras-chave: Controle de Tensão. Redes de Distribuição. Veículos Elétricos. OLTC. Fotovoltaica.

RESUMEN

Las redes de distribución activas con una alta penetración de energía fotovoltaica (PV), sistemas de almacenamiento de energía por batería (BESS) y recarga de vehículos eléctricos (EV) se enfrentan a importantes retos en materia de regulación de tensión y a un desgaste acelerado de los transformadores de tensión de paso (OLTC). Este artículo propone un marco coordinado de control de tensión multicapa que opera en múltiples escalas temporales. Integra un control local rápido de tipo «fuzzy» de voltaje-var y un control P/Q sensible al estado de carga a nivel del inversor/BESS, una conmutación coordinada intermedia de condensadores y un programador supervisor de los OLTC formulado como un problema de control predictivo de modelos (MPC). El sistema híbrido de bucle cerrado continuo-discreto resultante se evalúa mediante cosimulación en el dominio del tiempo en una red modificada de 13 buses del IEEE (IEEE 13-bus+SFVE) y en una red urbana real de 150 buses en Manaos (RDRM), bajo perfiles realistas de irradiación y carga. En el caso de la red IEEE de 13 buses+SFVE, el esquema redujo las infracciones de tensión en toda la red de distribución del 15,22 % al 4,83 % y las operaciones de conmutación del OLTC de 14 a 1 al día. En el caso del alimentador RDRM, las infracciones se redujeron del 72,44 % al 9,76 %, con una sola operación del OLTC en 24 horas, ambas sin restricción de la producción fotovoltaica. Esta contribución integradora demuestra mejoras sustanciales en la calidad de la tensión y en la vida útil del OLTC, lo que pone de relieve una vía práctica para la gestión activa de la red de distribución.

Palabras clave: Control de Tensión. Redes de Distribución. Vehículos Eléctricos. OLTC. Fotovoltaica.

INTRODUCTION

The increasing penetration of distributed photovoltaic (PV) generation and electric vehicles (EVs) is profoundly altering distribution network operation, introducing rapid power fluctuations and localized demand surges [1, 2].

These dynamics challenge traditional voltage regulation equipment, such as on-load tap changers (OLTCs) and capacitor banks, which were designed for more stable, unidirectional power flows. Over-reliance on these devices can lead to excessive operation, accelerating mechanical wear and increasing maintenance costs [3, 4].

Modern inverter-based distributed energy resources (DERs) and battery energy storage systems (BESS) offer new control capabilities by modulating reactive and active power [5, 6, 7]. The voltage sensitivity to active and reactive power injections in radial feeders can be approximated by:

$$\Delta V \approx \frac{R \cdot \Delta P + X \cdot \Delta Q}{V_{\text{base}}}, \quad (1)$$

where:

R and X are equivalent resistance and reactance,
ΔP and ΔQ are incremental active and reactive injections,
and V_{base} is the nominal voltage.

This relationship highlights the potential of reactive control and selective active power adjustments to manage voltage excursions while respecting inverter apparent power limits:

$$P^2 + Q^2 \leq S_{\max}^2. \quad (3)$$

Effectively leveraging these capabilities requires multi-timescale control strategies. Fast local actions from inverters address rapid disturbances, intermediate actions coordinate capacitor switching, and slower supervisory decisions manage OLTC tap changes to preserve equipment lifetime and en-sure long-term voltage compliance [3, 8, 9].

This study proposes a coordinated multi-layer voltage control framework that integrates:

1. Distributed adaptive fuzzy Volt–Var controllers at inverter/BESS level for fast local response;
2. Coordinated capacitor switching for intermediate corrective action;
3. A predictive supervisory OLTC scheduler formulated as a model predictive control (MPC) problem to minimize tap operations; and
4. A fuzzy logic PV curtailment module as a last resort under extreme over-generation.

The main strength of this work lies in the coordinated integration of these diverse control layers and device types into an operationally coherent frame-work for active distribution networks with high PV penetration. The approach respects practical constraints and is validated through co-simulation on a modified IEEE 13-bus feeder and a real 150-bus urban feeder in Manaus.

While the contribution is primarily integrative, we acknowledge existing gaps, including the need for formal hybrid-system analysis, comprehensive benchmarking against AC optimal power flow (OPF) and advanced dis-tributed controllers, and a more rigorous Monte Carlo-based uncertainty assessment.

The remainder of this paper is organized as follows. Section 2 reviews related work. Section 3 presents the system models and hybrid formulation. Section 4 details the hierarchical control architecture. Section 5 describes the simulation setup and metrics. Section 6 presents numerical results. Section 7 discusses strengths, weaknesses, and required extensions, and Section 8 concludes the paper.

RELATED WORK

Voltage regulation in active distribution networks with inverter-based resources and electric vehicles has received considerable attention in recent years [1, 2, 10, 8, 4]. Conventional OLTCs, capacitor banks, and voltage regulators often show limitations under the fast variability introduced by PV generation and EV charging [3, 11, 12].

Local rule-based Volt–Var control, commonly implemented in commercial inverters following standards like IEEE Std 1547–2018, maps local voltage measurements into reactive power commands [1, 5, 13]. A generic piecewise mapping is given by:

$$Q(V) = \begin{cases} Q_{\max}, & V \leq V_1 \\ aV + b, & V_1 < V < V_2 \\ Q_{\min}, & V \geq V_2 \end{cases} \tag{4}$$

Centralized OPF formulations and supervisory controllers can compute globally optimal setpoints for DERs and OLTCs, but they require accurate models and significant computational resources [9, 14, 4]. Distributed consensus-based and primal–dual algorithms, as well as hierarchical MPC, have been proposed to improve scalability [8, 4, 9].

BESS can provide both active energy shifting and reactive voltage support [7, 15]. Predictive OLTC scheduling and MPC techniques reduce unnecessary tapping by anticipating near-term PV and load variations [3, 9, 4]. Typical formulations minimize a weighted sum of voltage violation penalties and tap change costs over a finite horizon:

$$J = \sum_{k=0}^{H} \left[\omega_V \sum_{n} (V_n(k) - V_{\text{ref}})^2 + \omega_\tau \left| \Delta\tau(k) \right| \right]. \tag{5}$$

Fuzzy logic controllers are used for Volt–Var and hybrid P/Q control due to their tolerance to uncertainty and nonlinearities [16, 17, 18]. However, full documentation of rule bases and membership functions is not always provided, which can limit reproducibility.

Despite this literature, significant gaps remain. Few studies formulate a unified hybrid continuous–discrete model encompassing OLTCs, capacitors, inverters, and fuzzy logic. There is also a lack of formal stability analysis for hybrid multi-layer architectures combining MPC and fuzzy rules.

Many Monte Carlo studies report only average performance, without dispersion or worst-case behavior. Benchmarking against strong baselines such as AC OPF and centralized MPC is still sparse. The present work contributes an integrated, practically oriented hierarchical framework while explicitly recognizing that further theoretical developments are needed.

System Model and Hybrid Formulation

This section summarizes the network and component models and introduces a hybrid-system representation consistent with the hierarchical control architecture. Two distribution feeders are considered:

1. a modified IEEE 13-bus radial feeder adapted for high PV and EV penetration (IEEE 13-bus+SFVE), derived from [2], with PV, BESS, EV charging, OLTC, and capacitors;
2. a real Manaus urban feeder (RDRM) with approximately 150 buses at 13.8 kV, including heterogeneous loads, distributed PV, and EV charging.

Network lines are modeled by series impedance and, when relevant, shunt capacitance. Loads are represented as ZIP models with 5-minute resolution time series load shapes reflecting residential/commercial demand and EV charging patterns [19, 20, 21]. Distributed PV plants are modeled as inverterinterfaced units with active power following irradiance profiles and reactive control within capability curves. BESS units follow active/reactive capability constraints and SoC dynamics [7, 15].

At each bus n, the complex voltage is $V_n = |V_n|e^{j\theta_n}$, and the net complex power injection is:

$$S_n = P_n + jQ_n = S_n^{\text{load}} + S_n^{PV} + S_n^{BESS} + S_n^{EV}. \quad (5)$$

The power flow equations can be compactly written as:

$$\mathbf{S} = \text{diag}(\mathbf{V})\mathbf{Y}^*\mathbf{V}^*, \quad (6)$$

with bus voltage limits:

$$V_{\min} \leq |V_n| \leq V_{\max}, \quad \forall n. \quad (7)$$

Component Models

OLTC: The OLTC is modeled with discrete taps $\tau_{min}, \dots, \tau_{max}$, each yielding an effective ratio:

$$\alpha(\tau) = \alpha_0(1 + \Delta\alpha\tau), \qquad (8)$$

with mechanical constraints such as minimum time between operations and maximum daily operations [3, 4].

Capacitor banks: The switched capacitor banks at buses $i \in \beta_C$ are modeled as discrete reactive injections with hysteresis and dwell times:

$$Q_i^{\text{cap}}(t) = s_i(t)\,\bar{Q}_i, \qquad (9)$$

where:

s_i is a discrete step index.

PV inverters: Inverters obey the apparent power constraint in (2), with active power bounded by available irradiance. Local Volt–Var control or fuzzy logic modulates reactive support [1, 13, 18].

BESS: BESS units are modeled with active power control and reactive capability, subject to SoC dynamics and efficiency:

$$\text{SoC}_i(t+1) = \text{SoC}_i(t) - \frac{\Delta t}{E_{\text{rated},i}}\left(\eta_{\text{ch}} P_{\text{ch},i}(t) - \frac{1}{\eta_{\text{dis}}} P_{\text{dis},i}(t)\right) \qquad (10)$$

with:

SoC bounds $SoC_{i,min} \leq SoC_i(t) \leq SoC_{i,max}$.

Test Systems

IEEE 13-bus+SFVE Feeder

The first test system is a modified version of the IEEE 13-bus radial distribution feeder, extended to represent a highly active distribution network with significant penetration of distributed PV generation, BESS units, and EV charging infrastructure. The feeder diagram is shown in Fig. 1, and the main components are summarized in Table 1.

Real Distribution Network of Manaus (RDRM)

The second case study is based on a real medium-voltage urban distribution feeder located in the city of Manaus, Brazil, referred to as the Real Distribution Network of Manaus (RDRM). This feeder comprises approximately buses at 13.8 kV, supplied from a 69/13.8 kV, 10 MVA substation transformer equipped with an OLTC. The network features a main trunk with multiple lateral branches, two shunt capacitor banks for reactive support, and a heterogeneous portfolio of loads. In addition, the RDRM incorporates multiple PV plants and BESS units, as well as both slow and fast EV charging stations.

The main technical characteristics of the RDRM feeder are summarized in Table 2, while Fig. 2 provides a schematic layout of the buses, lines, and DER placements.

Figure 1. Diagram of the modified IEEE 13-bus+SFVE feeder showing PV units, BESS, EV charging stations, capacitor banks, and the substation OLTC transformer.

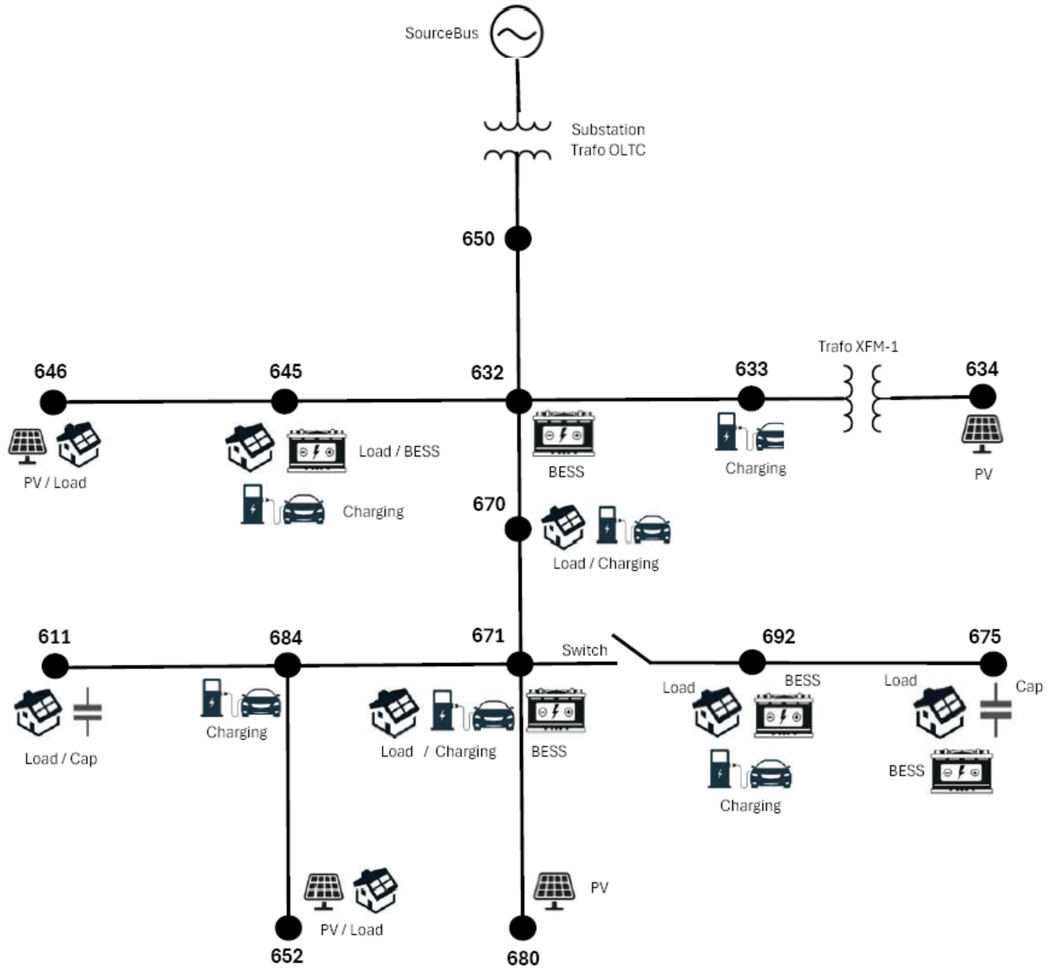

Source: Authors

Table 1. Summary of components in the modified IEEE 13-bus+SFVE feeder.

Component	Type / Description	Qty
Transformers	Substation OLTC 115/4.16 kV, 5 MVA, Δ–Y	1
	Distribution 4.16/0.48 kV, 0.5 MVA, Y–Y	1
Linecodes	3ϕ overhead (601, 602)	2
	2ϕ overhead (603, 604)	2
	1ϕ overhead (605, 607)	2
	3ϕ underground (606)	1
Buses	Total buses (incl. substation and LV)	15
Loads	Feeder loads (original/modified)	15
	EV slow charging (3ϕ, 22 kW each)	3
	EV fast charging (3ϕ, 50/100/150 kW)	3
Capacitors	3ϕ shunt caps (600 kVAr @ 675; 300 kVAr @ 611)	2
PV systems	100 kW @ 0.48 kV (bus 634)	1
	500 kW @ 4.16 kV (buses 646, 652, 680)	3
BESS units	450 kW / 700 kWh @ 4.16 kV (buses 632, 645, 671, 611, 675, 692)	6
EV charging	Slow: 3 × 22 kW; fast: 50–100–150 kW	6

Note: Total PV capacity: 1.6 MW. Total BESS power/energy: 2.7 MW / 4.2 MWh. Total EV peak demand: 366 kW.

Table 2. Technical summary of the modified Real Distribution Network of Manaus (RDRM).

Category	Item	Value
Network	Buses (approx.)	150
	Lines	96
	Primary voltage	69 kV
	Secondary voltage	13.8 kV
Transformer (OLTC)	Rating	69/13.8 kV, 10 MVA, 3-phase
Feeder	Length	≈ 12 km
	Peak demand	≈ 6.96 MW
PV generation	Units / Capacity	12 / 1.44 MW
BESS	Units / Capacity	6 / 2.70 MW
EV slow charging	Units / Capacity	10 / 220 kW
EV fast charging	Units / Capacity	5 / 0.58 MW
Capacitor banks	Units / Capacity	2 / 1050 kVAr

Source: Authors

Figure 2. Diagram of the modified Real Distribution Network of Manaus (RDRM) showing the 150-bus topology, DER placements, shunt capacitors, and EV charging infrastructure.

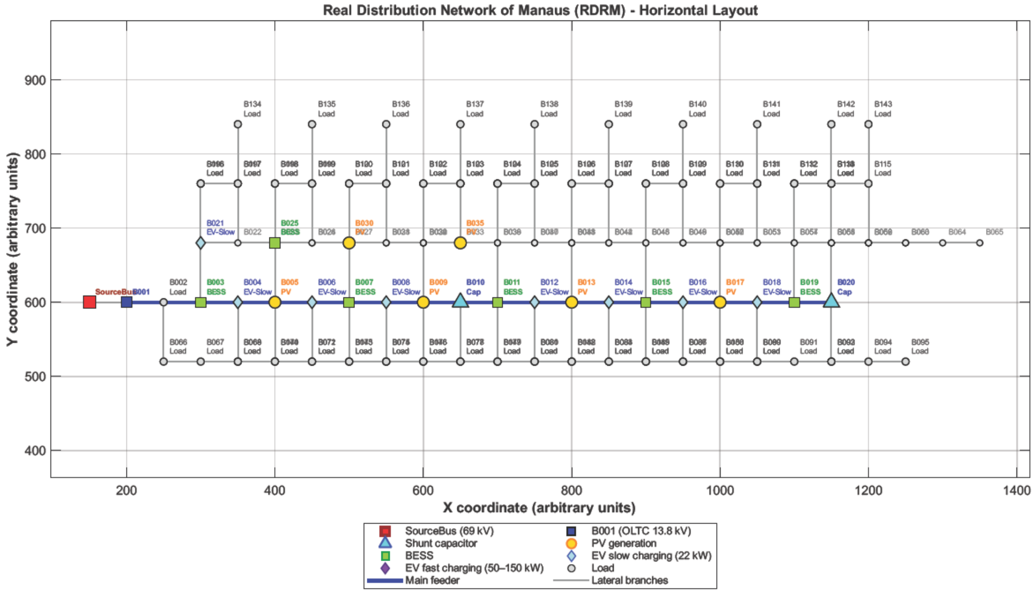

Source: Authors

Hybrid Closed-Loop Representation

Let X_C collect continuous variables (voltages, angles, and SoC) and X_d collect discrete variables (OLTC tap, capacitor states, and fuzzy modes/curtailment flags). Let u represent the control inputs. The closed-loop architecture can be abstracted as a hybrid system:

$$\dot{\mathbf{x}}_c = f_c(\mathbf{x}_c, \mathbf{x}_d, \mathbf{u}), \quad (11)$$

$$\mathbf{x}_d^+ = f_d(\mathbf{x}_c, \mathbf{x}_d), \quad (12)$$

whenever the guard conditions (voltage thresholds, timing logic, and MPC updates) are triggered.

Hierarchical Control Architecture

The proposed control architecture distributes responsibilities across three main layers: fast local inverter/BESS fuzzy control, intermediate coordinated capacitor switching, and slow predictive OLTC scheduling, complemented by a fuzzy PV curtailment module.

Fast Layer: Local Fuzzy Volt–Var and P/Q Control

At the fastest timescale, each inverter/BESS implements a fuzzy Volt–Var controller that adjusts reactive power $Q_i(t)$ and, when necessary, issues a soft active power curtailment command $P_{curt,i}(t)$ based on local measurements [16, 18, 15]. The inputs to this controller include the voltage error $e_i(t)$, its rate of change $\dot{e}_i(t)$, the BESS state of charge $SoC(t)$, the reactive power headroom $Q_{head,i}(t)$, and a normalized curtailed energy ratio $r_i(t)$:

$$e_i(t) = V_i(t) - V_{\text{ref}}, \quad (13)$$

$$\dot{e}_i(t) \approx \frac{e_i(t) - e_i(t - \Delta t)}{\Delta t}, \quad (14)$$

$$Q_{\text{head},i}(t) = \sqrt{S^2_{\max,i} - P^2_i(t)}, \quad (15)$$

$$r_i(t) = \frac{E_i^{\text{curt}}(t)}{E_i^{\text{avail}} \cdot (t + \varepsilon)}. \quad (16)$$

The fuzzy controller can be summarized as:

$$\Delta Q_i(t),\ P_{\text{curt},i}(t) = \mathcal{F}_i\left(e_i(t),\ \dot{e}_i(t),\ \text{SoC}_i(t),\ Q_{\text{head},i}(t),\ r_i(t)\right), \quad (17)$$

subject to the inverter apparent power constraint:

$$(P_i(t) - P_{\text{curt},i}(t))^2 + (Q_i(t) + \Delta Q_i(t))^2 \leq S^2_{\max,i}. \quad (18)$$

Figure 3. Block diagram of the local fuzzy controller with membership functions for voltage error ei and reactive power output ΔQ_i.

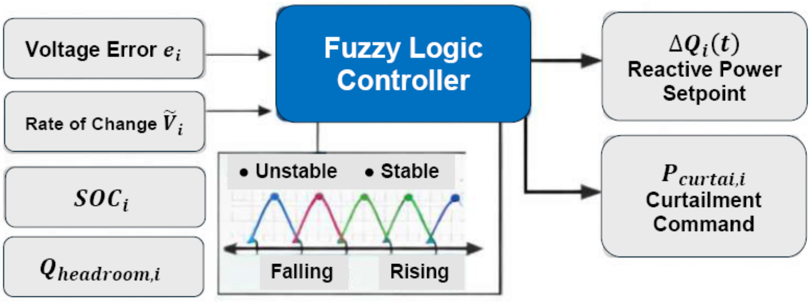

Source: Authors

Intermediate Layer: Coordinated Capacitor Switching

Capacitor banks operate at intermediate time scales to correct persistent deviations. Each capacitor uses hysteresis with a deadband $[V_{low}^{cap}; V_{high}^{cap}]$ and dwell times:

$$s(t) = \begin{cases} \text{OFF}, & \bar{V}_n(t) > V_{\text{high}}^{\text{cap}} \text{ for } \Delta t > T_{\text{delay}} \\ \text{ON}, & \bar{V}_n(t) < V_{\text{low}}^{\text{cap}} \text{ for } \Delta t > T_{\text{delay}} \end{cases} \quad (19)$$

where $\bar{V}_n(t)$ is the short-term averaged voltage. A supervisory capacitor coordinator aggregates local requests and solves a simple discrete optimization to minimize a mid-term cost:

$$J_{\text{cap}} = \omega_V^{\text{cap}} \sum_n \left(\bar{V}_n - V_{\text{ref}}\right)^2 + \omega_s^{\text{cap}} \sum_j \text{Cost}_{\text{sw}}(j), \quad (20)$$

subject to the step and dwell constraints.

Figure 4. Architecture of OLTC + Volt–Var co-simulation and capacitor coordination diagram.

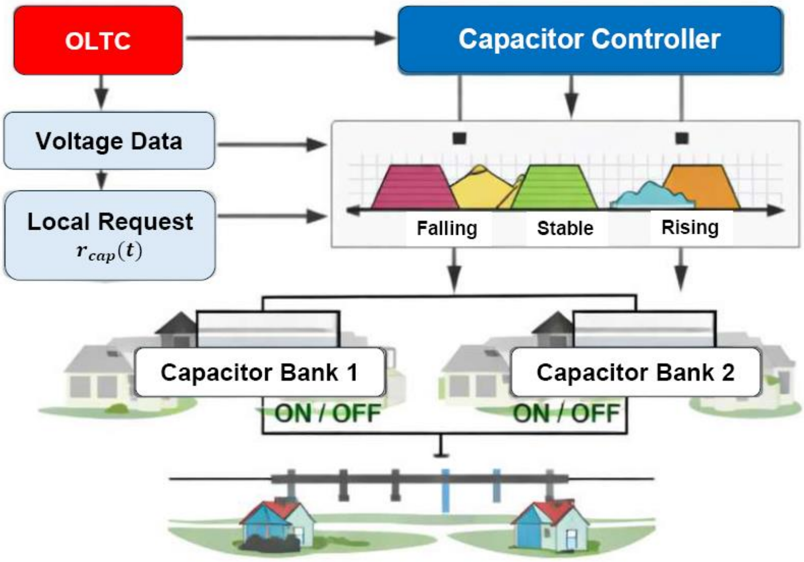

Source: Authors

Slow Layer: Predictive OLTC Scheduling (MPC)

The OLTC supervisor operates on the slowest time scale, using an MPC formulation:

$$\min_{\tau(k)} J_{\text{OLTC}} = \sum_{k=0}^{H} \left[\omega_V \sum_{n} (V_n(k) - V_{\text{ref}})^2 + \omega_\tau \left| \Delta\tau(k) \right| \right]. \tag{21}$$

subject to:

- power flow constraints (linearized or full AC);
- tap bounds $\tau_{min} \leq \tau(k) \leq \tau_{max}$, integer;
- mechanical constraints (minimum inter-tap time, daily limit).

Forecasted voltages Vn(k) incorporate the expected inverter/BESS responses and predicted capacitor states. Tap changes are penalized to avoid reacting to transients and to coordinate with lower layers.

Last-Resort Layer: Fuzzy PV Curtailment

When local reactive support and capacitors cannot avoid voltage violations under limited headroom, a fuzzy PV curtailment module issues graded active power reductions:

$$\min_{\Delta P_{\mathrm{curt},i}} \sum_i C_i \cdot \Delta P_{\mathrm{curt},i} \quad \text{s.t.} \quad V_n \in [V_{\min}, V_{\max}],\ \forall n \tag{22}$$

where:

C_i encodes the economic and technical priorities.

Coordination relies primarily on local measurements and low-bandwidth supervisory messages exchanged every 30–60 seconds. Local fuzzy controllers operate autonomously; if communication is lost or delayed, they revert to safe local behavior. The co-simulation and implementation details follow the OpenDSS–MATLAB/Simulink coupling described in the article.

Simulation Setup, Case Studies, and Metrics

The simulation environment employs a co-simulation approach, coupling a quasi-static power flow solver with control routines. The simulation horizon is 24 hours, with a 5-minute resolution (Δt = 5min, N = 288). Transient co-simulation steps are set between 0.1–1.0 s when necessary. Local fuzzy loops operate at 0.2–1 s, capacitor decisions at 10–60 s, and OLTC decisions at 60–300 s.

Table 3. Simulation parameters (summary).

Parameter	**Value / Description**
Simulation horizon	24 h
Quasi-steady resolution	5 min ($N = 288$ steps)
Transient co-simulation step	0.1–1.0 s (when required)
Control loop intervals	Fuzzy: 0.2–1 s; Capacitors: 10–60 s; OLTC: 60–300 s
Monte Carlo realizations (extended)	At least 100 recommended for robust statistics

Source: Authors

Table 4. Equipment and control parameters (representative).

Item	Value / Description
OLTC	17 taps (±8); step = 0.625% (≈ 0.00625 p.u.); band = 0.97–1.03 p.u.; hysteresis = 0.003 p.u.; minimum inter-tap = 5 min
Capacitor banks	IEEE13-SFVE: Bus 611 = 300 kVAr; Bus 675 = 600 kVAr; dwell = 30 s; RDRM: as per actual configuration
BESS units	Six units
PV units	Multiple distributed units with ratings per feeder layout
Fuzzy controller	Mamdani; inputs

Source: Authors

Table 5. Time series inputs (summary).

Category	Description
Load profiles	5-minute ZIP models; residential/commercial mixes; daily curves.
PV irradiance	Measured or synthetic profiles from INMET [18]; scaled to PV ratings [10], [30].
EV charging	Slow (7–22 kW) and fast (50–150 kW) chargers; stochastic arrival/departure and power classes inspired by [16], [17], [28], [29].
Disturbance cases	Cloud transients; EV clustering peaks.

Source: Authors

Performance Metrics

The main performance metrics are defined as follows.

Percentage of intervals outside [0.95, 1.05] p.u. (%out):

$$\%out = 100 \cdot \frac{1}{N \cdot N_b} \sum_{t=1}^{N} \sum_{n=1}^{N_b} I_n(t) \tag{23}$$

where:

$I_n(t) = 1$ if $V_n(t) \leq 0.95$ or $V_n(t) \geq 1.05\ p.u.$, else 0.

Minimum bus voltage (V_{min}):

$$V_{\min} = \min_{t,n} V_n(t). \tag{24}$$

OLTC tap changes per day (N_{tap}):

$$N_{tap} = \sum_{t=1}^{N-1} 1_{\tau(t+1)\neq\tau(t)} \tag{25}$$

Curtailed PV energy (E_{curt}):

$$E_{\text{curt}} = \sum_{t=1}^{N} \sum_{i\in PV} P_{\text{curt},i}(t)\,\Delta t. \tag{26}$$

Feeder energy losses (E_{loss}):

$$E_{\text{loss}} = \sum_{t=1}^{N} P_{\text{loss}}(t)\,\Delta t. \tag{27}$$

Fairness index (J_{fair}):

$$J_{\text{fair}} = 1 - \frac{\sigma(P_{\text{support}})}{\mu(P_{\text{support}})}, \tag{28}$$

Where

$P_{support}$ is the vector of aggregate support contributions by the DERs.

Table 6. Performance metrics (summary).

Metric	Description
%out	Percentage of time (or nodes) outside the admissible voltage band
V_{min}	Minimum nodal voltage observed over the simulation horizon
N_{tap}	Number of OLTC tap operations
E_{curt}	Total curtailed energy
E_{loss}	Total system energy losses
BESS SoC	Average state of charge and SoC constraint violations
J_{fair}	Fairness index among users, buses, or devices

Source: Authors

RESULTS

This section presents the numerical results obtained from the co-simulation studies, evaluating the performance of the proposed hierarchical control framework across different feeders and operating conditions.

IEEE 13-bus+SFVE Feeder

A comparison between the baseline and hierarchical controls is summarized in Table 7. The coordinated fuzzy OLTC+Volt–Var controller significantly improved voltage regulation, reducing feeder-wide voltage violations by approximately 68.3% and decreasing OLTC tap operations by approximately 92.9%.

Table 7. 24 h performance – IEEE 13-bus+SFVE.

Metric (24 h)	Unit	Without Control	With Control
%out (feeder-wide)	(%)	15.22	4.83
V_{min}	(p.u.)	0.943	0.949
V_{max}	(p.u.)	1.038	1.006
$\bar{V}$	(p.u.)	0.984	0.980
N_{tap}	(per day)	14	1
E_{curt}	(kWh)	0.000	0.000
BESS average SoC	(%)	26.28	13.68
J_{fair}	–	NaN	-0.015

Source: Authors

Figure 5. Voltage profile of critical busbars in IEEE 13-bus+SFVE (predictive OLTC+BESS P+Q adaptive).

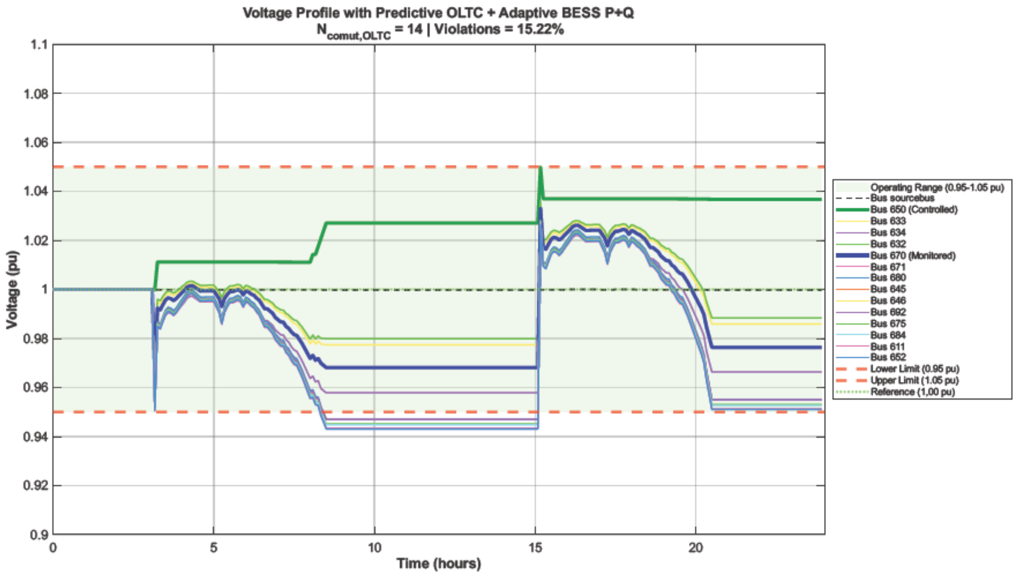

Source: Authors

Figure 6. Voltage profile of critical busbars in IEEE 13-bus+SFVE (coordinated fuzzy OLTC + Volt–Var).

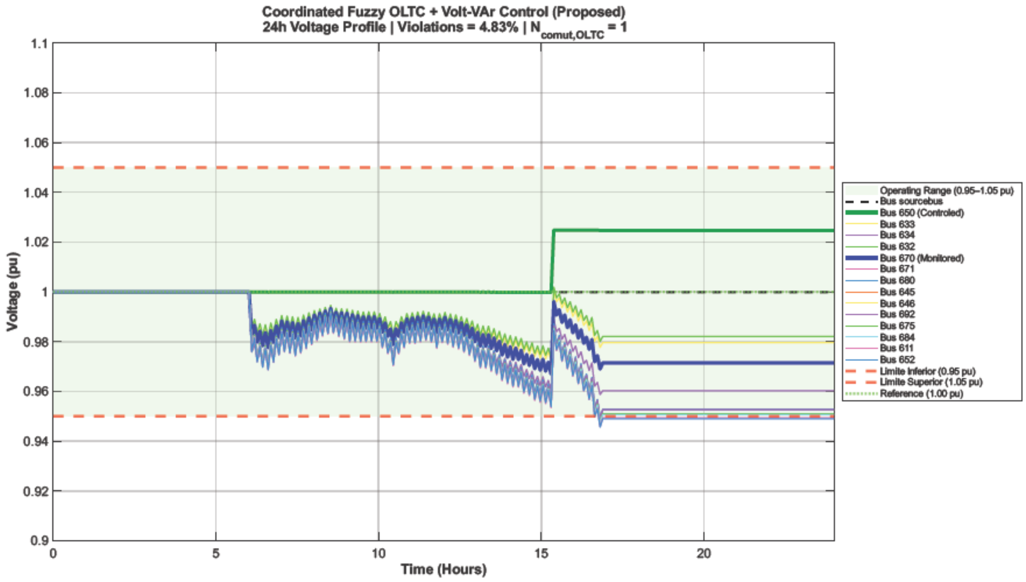

Source: Authors

Real Distribution Network of Manaus (RDRM)

For the RDRM feeder, the hierarchical control reduced feeder-wide voltage violations from 72.44% in the base case to 9.76%, increased the minimum voltage to 0.925 p.u., and raised the average feeder voltage to 0.976 p.u., with only one OLTC tap operation per day.

Computational Performance

The proposed OLTC MPC is formulated as a relatively small MIQP whose structure scales mainly with the prediction horizon and network size. The number of decision variables grows with the number of OLTC devices, while the number of constraints is dominated by bus-voltage and power-balance equations.

The current validation primarily compares the proposed hierarchical fuzzy-MPC architecture with a baseline no-hierarchy operation. However, a stronger benchmarking framework is required for future work to position the proposed scheme against modern optimal and distributed control methods, as well as regulatory baselines.

Table 8. 24 h performance – RDRM.

Metric (24 h)	Unit	Without Hierarchy	With Hierarchy
%out (feeder-wide)	(%)	72.44	9.76
$V_{\min}$	(p.u.)	0.908	0.925
$V_{\max}$	(p.u.)	0.985	1.018
$\bar{V}$	(p.u.)	0.938	0.976
N_{tap}	(per day)	0	1
E_{curt}	(kWh)	NaN	0.000
BESS average SoC	(%)	20.00	20.00
J_{fair}	–	NaN	NaN

Source: Authors

Figure 7. Voltage profile along the main trunk of RDRM without advanced control.

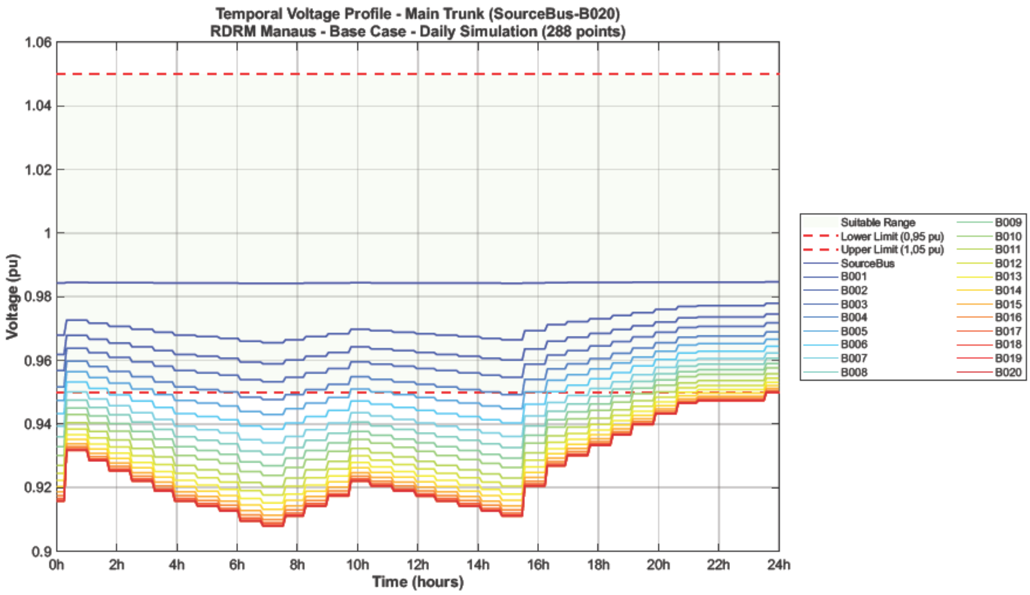

Source: Authors

Figure 8. Voltage profile along the main trunk of RDRM with the proposed coordinated control.

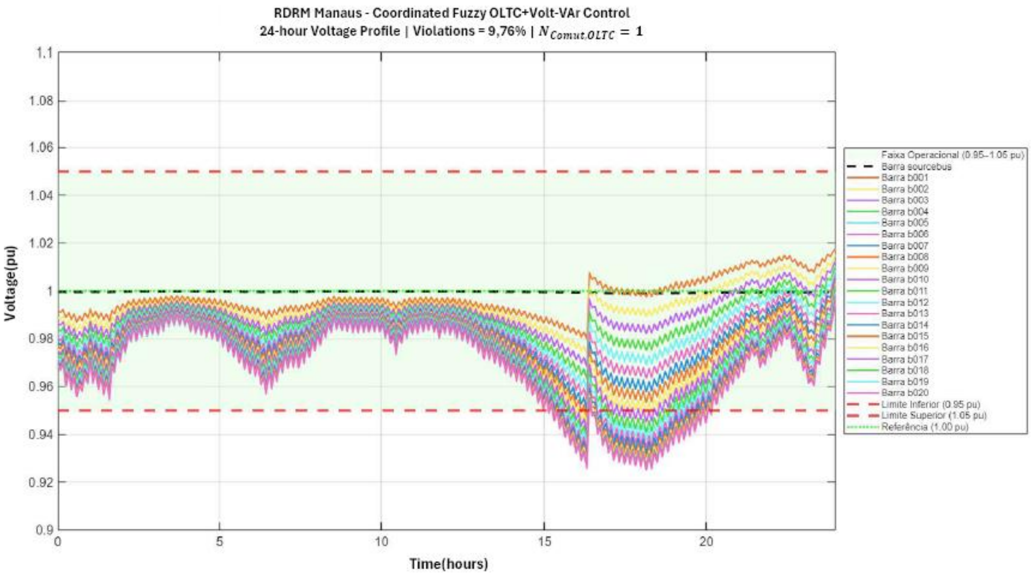

Source: Authors

Figure 9. RDRM 24 h voltage heatmap comparison: without control versus with proposed hierarchical control.

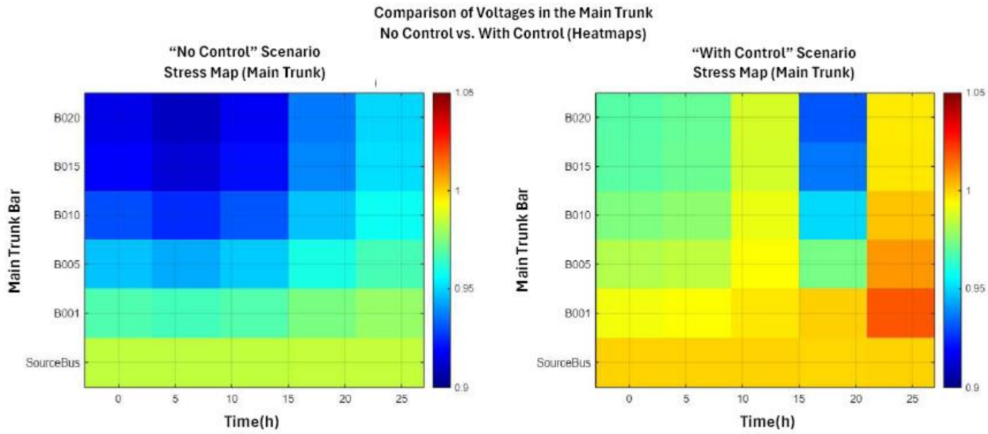

Source: Authors

Table 9. Typical growth of MPC problem size with network scale.

Network scale	N_b **buses**	$N_{\mathbf{var}} \approx HN_\tau$	$N_{\mathbf{con}} \propto HN_b$
Small	13	$O(H)$	$O(13H)$
Medium	150	$O(H)$	$O(150H)$
Large	500	$O(H)$	$O(500H)$

Source: Authors

Table 10. Processing time for 24 h co-simulations.

Feeder	Without Control (s)	With Control (s)
IEEE 13-bus+SFVE	18.41	24.91
RDRM ($\approx$ 150 buses)	43.88	46.42

Source: Authors

Table 11. Measured and extrapolated MPC execution times per step for a 24 h horizon.

Feeder	N_b	N_{step}	T_{24h} (s)	$\bar{T}_{\text{step}}$ (s)
IEEE 13-bus+SFVE	13	288	24.91	0.087
RDRM	150	288	46.42	0.161
Large feeder	500	288	101.37	0.352

Source: Authors

DISCUSSION

The proposed framework demonstrates effective multi-timescale coordination across fuzzy local control, capacitor switching, and MPC-based OLTC scheduling. It provides strong voltage quality improvements in both a standard test feeder and a real Brazilian urban network, while drastically reducing OLTC wear.

Several limitations are explicitly acknowledged:

- Formal stability analysis: A rigorous hybrid-system stability proof for the combined MPC + fuzzy architecture is still lacking.
- Benchmarking: The current comparison is limited to a no-hierarchy baseline. Future work should include AC OPF, primal–dual distributed controllers, and centralized MPC.
- Monte Carlo uncertainty: A statistically robust MC assessment is identified as a natural extension.
- Loss analysis: A comprehensive evaluation of how the hierarchical scheme affects network losses is deferred to future work.

CONCLUSION

This paper presented a coordinated multi-layer voltage control framework for active distribution networks, integrating fast local fuzzy Volt–Var control, intermediate capacitor switching, and a supervisory OLTC scheduler based on Model Predictive Control. The framework was validated via time-domain co-simulation on both the IEEE 13-bus+SFVE test feeder and the real 150-bus RDRM feeder in Manaus under realistic operating conditions.

Key results include:

- Voltage violation reduction from 15.22% to 4.83% (IEEE 13-bus+SFVE) and from 72.44% to 9.76% (RDRM);
- OLTC tap operations reduced from 14 to 1 per day;
- Zero PV curtailment under the tested scenarios;
- All 24 h simulations completed in under one minute, demonstrating computational suitability for quasi real-time deployment.

The integrative approach proves highly effective in balancing voltage quality, equipment longevity, and renewable energy utilization, offering a practical pathway for active distribution network management.

CREDIT AUTHOR STATEMENT

Weverson Cirino: Conceptualization, Methodology, Software, Validation, Formal analysis, Writing – original draft, Visualization.
Thiago Soares: Supervision, Writing – review and editing, Resources.
Israel Gondres Torné: Supervision, Project administration, Funding acquisition, Writing – review and editing.

DECLARATION OF COMPETING INTERESTS

The authors declare that they have no known competing financial interests or personal relationships that could have appeared to influence the work reported in this paper.

FUNDING

This research did not receive any specific grant from funding agencies in the public, commercial, or not-for-profit sectors.

DATA AVAILABILITY

Data will be made available on request.

DECLARATION OF GENERATIVE AI AND AI-ASSISTED TECHNOLOGIES IN THE MANUSCRIPT PREPARATION PROCESS

During the preparation of this work the author(s) used generative AI tools in order to assist with drafting, structuring, and language refinement. After using these tools, the author(s) reviewed and edited the content as needed and take full responsibility for the content of the published article.

ACKNOWLEDGEMENTS

The authors gratefully acknowledge the University of the State of Amazonas (UEA), and especially its Rector, for the favorable conditions provided for the development of this work, and the Graduate Program in Electrical Engineering (PPGEE) of the Institute of Technology (ITEC) at the Federal University of Pará (UFPA) for the opportunity to pursue doctoral studies in Electrical Power Systems. Special thanks are due to Prof. Dr. Thiago Mota Soares and Prof. Dr. Israel Gondres Torné, Senior Member, IEEE, for their invaluable guidance, insightful suggestions, and careful corrections, which substantially improved this manuscript.

REFERENCES

[1] IEEE Power & Energy Society, IEEE Std 1547-2018, Standard for Interconnection and Interoperability of Distributed Energy Resources with Associated Electric Power Systems Interfaces, https://standards. ieee.org/ieee/1547/5915/, accessed: 15 May 2024 (2018).

[2] W. H. Kersting, Radial distribution test feeders, IEEE Transactions on Power Systems 6 (3) (1991) 975–985. doi:10.1109/59.119237.

[3] O. D. Melgar-Domínguez, P. Aristidou, *et al.*, On-load tap-changer op eration and coordination in distribution networks with high der penetration, IET Generation, Transmission & Distribution 16 (12) (2022) 2456–2468. doi:10.1049/gtd2.12420.

[4] F. Liu, *et al.*, Coordinated control of on-load tap changer and distributed resources for voltage regulation in active distribution networks, Electric Power Systems Research 195 (2021) 107211. doi:10.1016/j.epsr.2020.107211.

[5] F. Blaabjerg, R. Teodorescu, M. Liserre, A. V. Timbus, Overview of control and grid synchronization for distributed power generation systems, IEEE Transactions on Industrial Electronics 53 (5) (2006) 1398–1409. doi:10.1109/TIE.2006.881997.

[6] M. Liserre, F. Blaabjerg, *et al.*, Stability of photovoltaic inverters in autonomous operation, IEEE Transactions on Power Electronics 30 (12) (2015) 6759–6770. doi:10.1109/TPEL.2014.2384033.

[7] P. Gupta, S. Singh, D. Chauhan, Battery energy storage management for voltage support in pv integrated distribution systems, International Journal of Electrical Power & Energy Systems 149 (2023) 109002. doi: 10.1016/j.ijepes.2022.109002.

[8] L. Che, *et al.*, Coordinated volt/var control with oltc and distributed resources in active distribution networks, Electric Power Systems Research 215 (2023) 108120. doi:10.1016/j.epsr.2022.108120.

[9] T. Tewari, A. Mohapatra, S. Anand, Coordinated control of oltc and energy storage for voltage regulation in distribution network with high pv penetration, IEEE Transactions on Sustainable Energy 12 (1) (2021) 262–272. doi:10.1109/TSTE.2020.2991017.

[10] L. Che, Y. Zhang, Y. Weng, *et al.*, Voltage regulation in distribution networks with high der penetration: Challenges and solutions, IEEE Transactions on Power Delivery 38 (2) (2023) 789–802. doi:10.1109/TPWRD.2022.3211088.

[11] A. Chakraborty, S. Banerjee, N. Das, Performance assessment of volt–var-based reactive power management in active distribution networks, Renewable Energy 190 (2022) 56–68. doi:10.1016/j.renene.2022.02.067.

[12] S. Habib, *et al.*, Impact of electric vehicle charging on distribution power networks: A review, Renewable and Sustainable Energy Reviews 81 (2018) 2002–2016. 340 doi:10.1016/j.rser.2017.06.079.

[13] Y. Zhang, H. Kim, J. Park, Adaptive volt–var curve design for pv inverters under unbalanced conditions, Energies 14 (12) (2021) 3629. doi:10.3390/en14123629.

[14] Y. Huo, *et al.*, Data-driven coordinated voltage control method of distribution networks with high dg penetration, IEEE Transactions on Power Systems 38 (2) (2023) 1543–1557. doi:10.1109/TPWRS.2022.3172667.

[15] C. P. Camillo, C. Cappellini, E. Santos, Adaptive fuzzy control for voltage regulation in smart grids, Electric Power Systems Research 211 (2022) 108622. doi:10.1016/j.epsr.2022.108622.

[16] J. M. Mendel, Uncertain Rule-Based Fuzzy Systems: Introduction and New Directions, 2nd Edition, Springer, 2017. doi:10.1007/978-3-319-51370-6.

[17] M. F. Mendonça, L. R. Santos, R. G. Vieira, Fuzzy-based voltage regulation in distribution feeders with distributed generation, SBA: Controle & Automação 32 (2) (2021) 215–229. doi:10.1590/0103-6513.20210116.

[18] D. Melgar-Domínguez, *et al.*, Coordinated fuzzy logic control for distributed pv inverters in active distribution networks, Electric Power Systems Research 205 (2022) 107739. doi:10.1016/j.epsr.2021.107739.

[19] J. A. P. Lopes, F. J. Soares, P. M. Almeida, Integration of electric vehicles in the electric power system, Proceedings of the IEEE 99 (1) (2011) 168–183. doi:10.1109/JPROC.2010.2066250.

[20] M. Rahman, *et al.*, Electric vehicle integration into power grids: A comprehensive review, IEEE Access 8 (2020). doi:10.1109/ACCESS. 2020.2973114.

[21] M. Steinmetz, *et al.*, Stochastic modeling of ev charging demand, Electric Power Systems Research 189 (2020) 106603. doi:10.1016/j.epsr. 2020.106603.